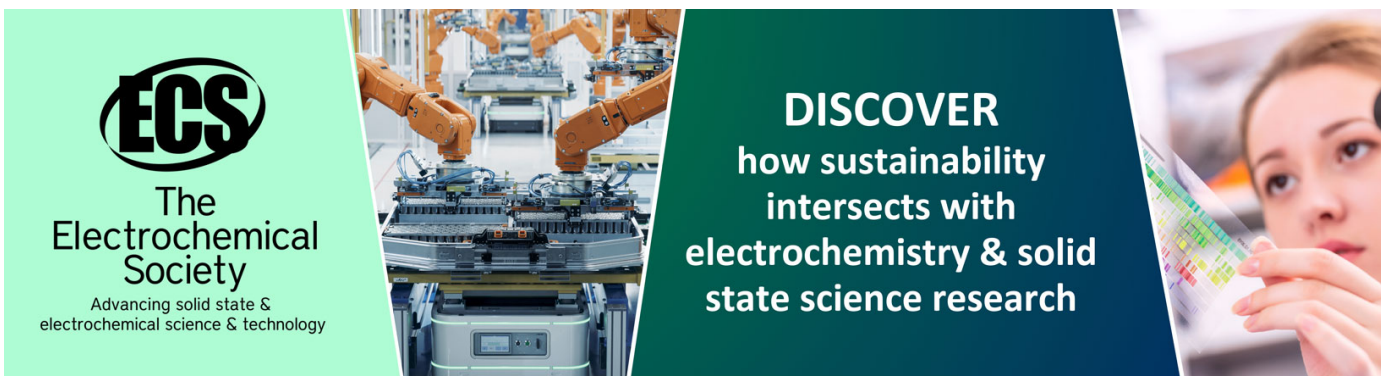**PAPER • OPEN ACCESS**

Accuracy in evaluating heat transfer coefficient by RANS CFD simulations in a rectangular channel with high aspect ratio - Part 2: channel with ribbed walls

To cite this article: Maria Corti *et al* 2023 *J. Phys.: Conf. Ser.* **2509** 012010

View the article online for updates and enhancements.

Accuracy in evaluating heat transfer coefficient by RANS CFD simulations in a rectangular channel with high aspect ratio – Part 2: channel with ribbed walls

Maria CORTI, Pasqualino GRAMAZIO, Damiano FUSTINONI, Luigi VITALI, and Alfonso NIRO*

Politecnico di Milano, Department of Energy
via Lambruschini 4, 20156 Milano, Italy

* Corresponding author e-mail: alfonso.niro@polimi.it

Abstract. In this paper, a Computational Fluid-Dynamics (CFD) analysis on heat transfer characteristic using Reynolds Averaged Navier-Stokes (RANS) equations on a rectangular channel with ribbed surfaces is presented. Several numerical simulations have been carried out on convective heat transfer of an air flow through a rectangular channel of 1:10 aspect ratio, 120 mm wide, 840 mm long, with 90° ribs. Ribs have a square cross section with 4 mm side and three different values of dimensionless pitch, namely, 10, 20 and 40. Results on convective global heat transfer coefficient, i.e., averaged over the whole channel, have been compared to experimental data obtained in a channel with the same geometry and boundary conditions. Agreement between numerical and experimental data is discussed for the three different pitches considered. As expected, comparisons show a decreasing reliability for increasing complexity. The aim of this work is to find a suitable configuration of a CFD model with RANS that will permit authors to apply it to the range of dimensionless pitches.

Key Words: *forced convection, heat exchanger, rectangular channel, ribbed surfaces, experimental tests, CFD validation, RANS*

1. Introduction

Heat transfer enhancement in air forced convection, specially associated to forced convection inside rectangular channels with various ribbed surfaces, sees a wide range of applicability in engineering applications. Thinking about applicability, in addition to the well-known use for cooling blades gas turbines [1], nuclear reactors and solar collectors [2,3], a novel challenging application is for automotive batteries cooling [4] which requires large contact area and very small height resulting thus in channel with high aspect ratio. What is peculiar in using ribs is they can be used as turbulence promoters to increase heat transfer in ducts while varying their pitch-to-rib-side ratio, cross section, or blockage ratio. At the ThermALab laboratory at Politecnico di Milano, authors have been and are currently involved in experimental analysis on fluid-dynamics and heat transfer characteristic of forced convection inside a channel with an aspect ratio of 1:10 [5-8]. Since it isn't always possible to test new configurations in the experimental apparatus, an ideal alternative is the use of Computational Fluid-Dynamics (CFD) methods applied on a three-dimensional domain. CFD is an effective tool for

investigations of fluid flow in ducts with rib roughened walls. As reported in [9], using finite volume CFD code, RANS turbulence models usually show good agreement with experimental results but it's necessary to highlight that the only use of RANS is not exhaustive and could be inaccurate with respect to other more computational-expensive turbulence models. In this work authors are looking for a CFD model using the RANS k-ω-SST model, widely chosen in literature for similar cases [10-12] with respect to k-ω, k-ε RNG, or k-ε Realizable models. In this paper, results on convective global heat transfer coefficient i.e., averaged over the whole channel, are presented discussing the comparison between experimental and numerical data for different configurations considered. The aim of this work is to find a suitable configuration of a CFD model with RANS that will permit authors to apply it to the range of dimensionless pitches.

2. Problem configuration and setup

2.1. Experimental set-up
The experimental set-up is described in detail in [5], briefly it consists in a rectangular channel of 1:10 aspect ratio with 90° staggered ribs on the upper and the lower walls.
A schematic view of the section dedicated to measurements is presented in Figure 1, and in Table 1 the main geometric parameters are summarized.
In this paper, the upper and the lower surfaces of the channel are characterized by the presence of ribs with squared cross section, having a section side s of 4mm. Ribs are 90° tilted with respect to the stream flow. The pitch-to-side ratio p/s considered have been 10, 20 ,40. They are staggered each other in each configuration considered in this study. The experimental channel operates with lower and upper walls maintained at fixed temperature, while side walls are adiabatic. The air flows at Reynolds number ranging from 700 to 8000, in this specific study Reynolds 7552 has been chosen. For simplicity the tree configurations considered will be named p10s4, p20s4, p40s4 as can be seen in Figure 2.

2.2. Numerical procedure
Numerical simulations have been carried out using the software Ansys Fluent 19.1 based on finite volume method. The solution domain is a 3D channel with a rectangular cross section as described previously. The working fluid is air, incompressible, with constant specific heat coefficient.
The solution domain also includes two added domains: one dedicated to the entrance and one dedicated to the outlet. This configuration, especially while dealing with geometries with obstacles, is recommended to avoid problems with reverse flows. Indeed, to ensure the re-arranging of the flow after the obstacle, the length required is typically 8 to 10 times the obstacle height [13].
The fluid flow inside the rectangular channel has been analysed at Re 7552 and under these applied working conditions the regime of the fluid flow is turbulent. For this reason, the mesh adopted is suitable for the analysis of a turbulent flow. It ensures a $y^+ = 1$ at the wall to solve the laminar sublayer.
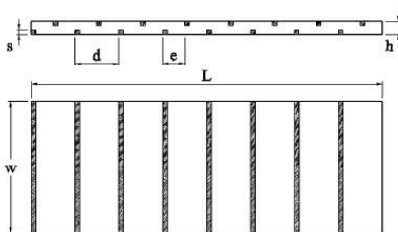

Figure 1. Ribbed channel geometry.

Table 1. Main channel parameters.

Main channel parameters	
Channel height, 2b=h	12.0 mm
Channel width, 2a=w	120.0 mm
Channel length, L	840.0 mm
Hydraulic diameter, D_h	21.82 mm

To obtain a grid independent solution has been carried out a sensitivity analysis. Since it is a three-dimensional case, given the three directions x, y, z where x is the direction of the channel width, y the direction of the channel height and z the streamwise direction, a sensitivity analysis has been carried out for each dimension. It has been observed that the impact of the sensitivity analysis on the solution is higher for the y-direction. Summarizing, various grids with number of elements ranging from $30 \cdot 10^6$ to $90 \cdot 10^6$ have been tested and the grids chosen for the discretization of the computational domain have around $65 \cdot 10^6$ number of elements. An overview of the grid can be seen in Figure 3 while the main quality parameters of the mesh as aspect ratio, orthogonal quality and skewness can be seen in Table 2.

2.3. Boundary conditions

Since the flow in the experimental set-up, at the inlet of the measurement section, can be considered hydrodynamically fully developed, this condition is required at the inlet of the present computational domain. At this scope a preliminary CFD simulation has been used. Considering an adiabatic channel with the same rectangular cross section, without ribs and enough long in the streamwise direction to guarantee the hydrodynamic development ($x_{fd,h} \geq 10 D_h$), it has been used to allow the fully development of the air flow. The velocity profile (its three components), and the corresponding turbulence parameters (Turbulent Kinetic Energy, k [m^2/s^2] and Specific Dissipation Rate, ω [1/s]) obtained at the outlet of this preliminary channel have been used as inlet condition for the analysed cases.
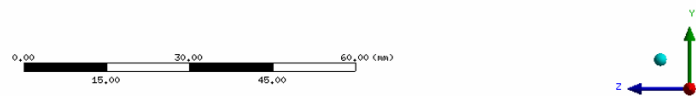

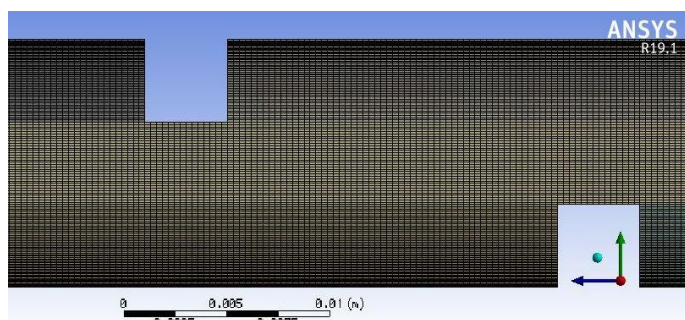**Figure 2.** Channel configurations considered.

Figure 3. Mesh overview.

Table 2. Mesh parameters.

Mean value of mesh parameters	
Skewness	1.9 e-2
Orthogonal	0.9836
Aspect Ratio	6.9
Element Quality	0.31448

Boundary conditions can be summarized as follow:
- Inlet: velocity inlet (fully developed velocity profile, previously generated) basing on the selected Reynolds number. The working fluid is air, enters the channel at uniform temperature, $T_{in} = 296K$. The fluid flow is not thermally developed yet, so temperature will develop inside the considered channel.
- Outlet: pressure outlet $P_{out} = 0Pa$.
- Wall: no-slip velocity condition is applied for all walls, moreover walls (upper, lower, and lateral) are heated at constant temperature, imposing $T_w = 323.15K$.
- Walls of ribs: no-slip velocity condition is applied, and these walls are considered adiabatic, imposing $\dot{q} = 0\,W/m^2$.
- Symmetry: since it can be considered a symmetric case in the x-direction (spanwise), symmetry has been applied at the wall identified from the centreline.

An additional clarification is needed for motivating the choice of setting all the walls of the channel as heated walls while in the experimental setup the lateral walls are considered adiabatic. Previous simulations [14] have been carried out to choose the most suitable boundary condition for numerical problem able to correctly represent the experimental configuration.

2.4. Solver setting and models

Semi-Implicit Method for Pressure Linked Equation-Consistent (SIMPLEC) algorithm is used for pressure-velocity coupling. This choice has been preceded by a comparison of other algorithms, i.e., Coupled and SIMPLE, but they had not managed the simulation to converge, or at least to converge to an unacceptable value of continuity residual in reasonable time.

The presented turbulent flow has been solved with RANS, choosing the k-ω-SST model. This choice has been motivated by evidence in literature and by previous analysis [14].

In literature k-ω-SST and k-ε-RNG models are the mostly used between turbulence models for simulations that required good agreement with experimental results [9]. k-ω-SST uses as default the Enhanced Wall Treatment, a wall function for the near-wall region i.e., viscous sublayer, buffer region and fully turbulent outer region.

Computational time has been considerable, about 96 hours of calculations per each single simulation using 25-30 cores Intel(R) Xeon(R) Gold 6148 CPU @ 2.40GHz.

RANS simulations stop when the continuity residual is lower than $1 \cdot 10^{-4}$.

3. Results

The number of Reynolds considered in this study has been precisely 7552. The choice of this value of Reynolds number is motivated by the fact that according to previous analyses [14] is shown that the accuracy of the solution of a RANS k-ω-SST simulation is better for Reynolds higher than 5000, and the value of 7552 is the highest Reynold number tested experimentally for channels with the three configurations proposed in this paper.

Per each configuration considered (p10s4, p20s4, p40s4) a CFD simulation has been carried out analysing in particular the agreement of heat transfer coefficients of numerical results with experimental data. The experimental data considered can be found in [5]. Values of the average Nusselt number vs Reynolds number for staggered transverse-ribs at different values of dimensionless pitch and height are presented in Figure 7, reference [5]. Values of friction factor vs Reynolds number for transverse-ribs in staggered arrangements at different values of dimensionless pitch and height are presented in Figure 5, reference [5], instead.

3.1. Convective heat transfer coefficient

Some sections, equidistant from each other, have been built along the entire channel to calculate the local heat transfer coefficient. For each section, of which an example can be seen in Figure 4, bulk temperature T_b and heat flux $\dot{q}$ have been calculated as mean section variables, from which can be computed the local convective heat transfer coefficient $h_z = \dot{q}_z/(T_w - T_b)$ and consequently the related

Nusselt number at any section $Nu_z = h_z D/k$. Values of the local convective heat transfer coefficients obtained section by section are shown in the graph in Figure 5. The presence of ribs shows a significant change in the trend only for the configuration of p10s4, for other configurations the trend is the one of a channel with plane walls, but with an increase in convective heat transfer coefficient.

By way of example, a velocity and a temperature contour, plotted over a section at z = 0.402 m for channel p20s4, are proposed in Figure 6 and Figure 7 respectively.

Experimentally, the mean convective heat transfer coefficient is calculated as $h_m = \dot{m}c_p(T_{out} - T_{in})/A/\Delta T_{m,ln}$ and the associated Nusselt number is $Nu_m = h_m D/k$ [5]. So, as first comparison, comparing mean convective heat transfer coefficients calculated according to the same formula, errors between experimental measurements and numerical results are around 16% for all the cases considered, showing that the CFD model underestimates the mean convective heat transfer coefficient measured experimentally, probably also due to assumptions made.

But regarding the overall average convective heat transfer coefficient, it can be also computed as follows, applying equation (1), for a more comprehensive evaluation of $\bar{h}$, which considers per example effects of the channel entrance and what happens along the entire length analyzed.

$$\bar{h} = \frac{1}{\sum \Delta A_z} \left(\sum_{z=1}^{n_{sections}} h_z \Delta A_z \right) \qquad (1)$$

According to equation (1), each contribution of the local convective heat transfer coefficients h_z has been weighed on the affected heat transfer surface ΔA_z and sum them up. Note that the value of the proposed $\bar{h}$ is independent of the number of sections considered (in this study $n_{sections} = 42$), since once 38 cutting sections are exceeded, the value of the average convective heat transfer coefficient is no longer influenced by the number of cutting planes chosen.
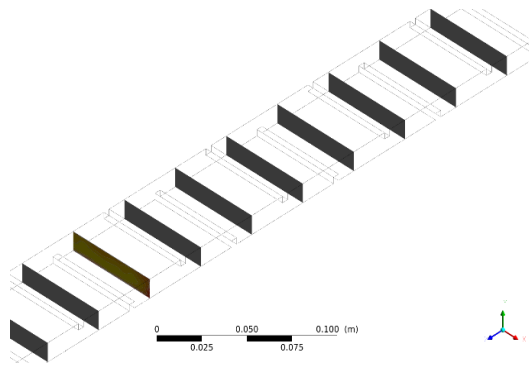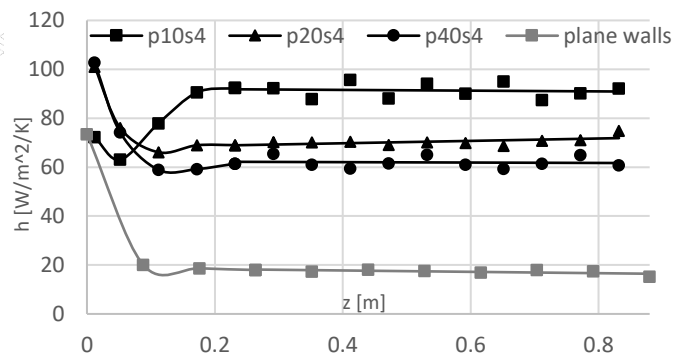

Figure 4. Exemplary section-planes.
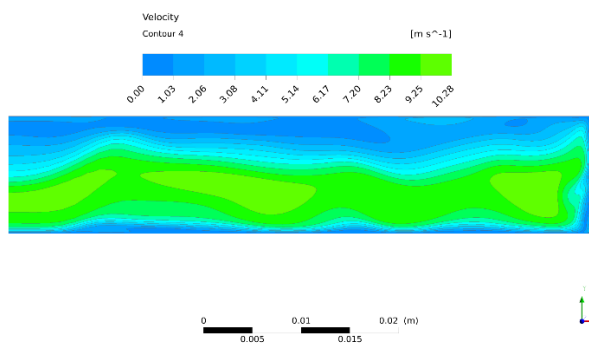

Figure 5. Heat transfer coefficient.

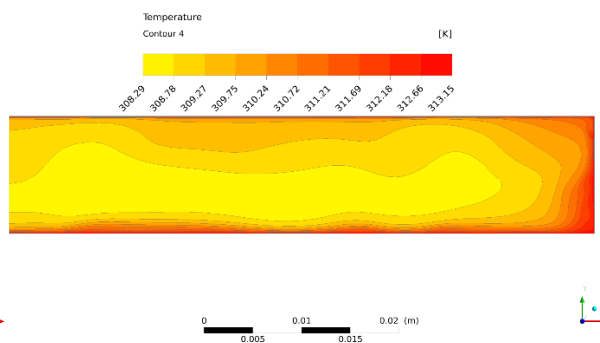**Figure 6.** Velocity contour on section plane at z = 0.402 m (p20s4 channel).

Figure 7. Temperature contour on section plane at z = 0.402 m (p20s4 channel).

Comparing the agreement of $\bar{h}$ with experimental results, the average convective heat transfer coefficient calculated for p40s4 configuration has the best behaviour, with an error of 8.8%. A little less agreement is given by p20s4 configuration with an error of 13.2%, followed by p10s4 configuration with an error of 20.4%. These results are presented graphically in Figure 8 and Figure 9. This can be due to the complexity of the flow since is shown increasing error at lower dimensionless pitch, where the flow is forced to pass in a more complex channel.

Finally, assuming $\bar{h}$, calculated according to eq. (1), as the real value and comparing it with h_m obtained numerically, it could be stated that experimental measurements tend to overestimate the mean convective heat transfer coefficient of the channel by 5-10% depending on the channel configuration.

Looking at the velocity contours in Figure 10, presence of a clockwise recirculating vortex is predicted. These vortexes are present in the low-pressure region between two ribs. Another observable factor is related to blockage effects of ribs in the channels. The flow velocity is higher in the centre of the channel in p10s4 configuration as the available section is reduced.

3.2. Pressure Drops

Friction factors obtained from pressure drops deriving from numerical results through equation (2) have been compared with experimental values, available only for dimensionless pitches of 20 and 40.

$$f_{Darcy} = \left(\Delta P_0 / 0.5\rho u^2\right)(D_h/L) \qquad (2)$$

Error between numerical and experimental values [5] has been 11% for a dimensionless pitch of 20 ($f_{Darcy\text{-}CFD} = 0.495$, $f_{Darcy\text{-}Exp} = 0.444$) and 9% for a dimensionless pitch of 40 ($f_{Darcy\text{-}CFD} = 0.238$, $f_{Darcy\text{-}Exp} = 0.218$).

4. Conclusion

In this paper the CFD model built for a high aspect ratio rectangular channel with 90° staggered ribs on upper and lower walls is presented. k-ω-SST RANS model has been chosen and the agreement with experimental data is good both at fluid-dynamic and thermal level with increasing error at lower dimensionless pitch, where the flow is forced to pass in a more complex channel.

This model has been built as a starting point to be able to expand the thermo-fluid dynamics study of high aspect ratio channels in presence of 90° ribbed surfaces in the range of dimensionless pitches considered without the need of carry out several experimental measurements. CFD could be considered as a helpful tool for the prediction of heat transfer coefficients in rib-roughened channels with 90° ribs, especially during early design-phases of parametric studies.

For more complex configurations which induced more complex flow structures, use of RANS could be not enough accurate, and so further analysis on these configurations will be carried out by exploiting LES to resolve at least larger scale structures.
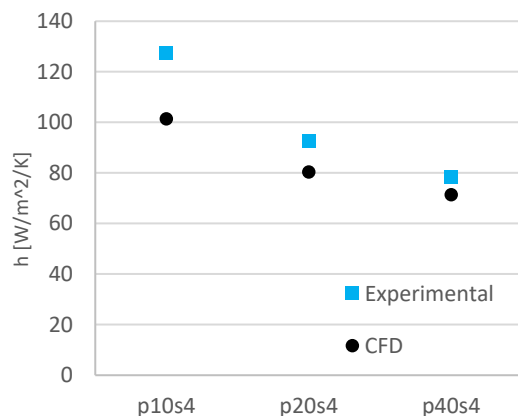

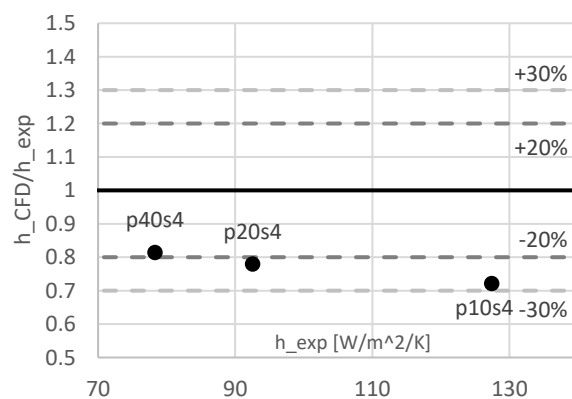**Figure 8.** Comparison of global heat transfer coefficient, experimental data versus CFD data.

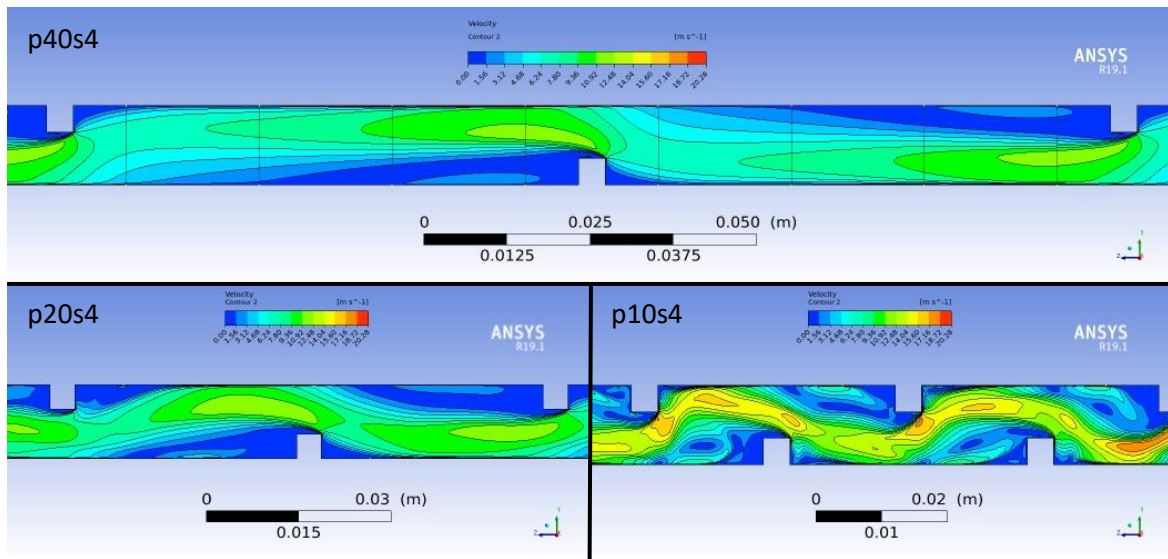**Figure 9.** Error between experimental and numerical $\bar{h}$ values.

Figure 10. Velocity contours taken on the symmetry plane of the channels considered.

Nomenclature

Symbol	Quantity	SI Unit
A	Area	m^2
a	Channel half width	m
b	Channel half height	m
h	Convective heat transfer coefficient	$W/m^2/K$
k	Thermal conductivity	W/m/K
k	Turbulent kinetic energy	m^2/s^2
L	Channel length	m
$\dot{m}$	Mass flow rate	kg/s
Nu	Nusselt number	-
P	Pressure	Pa
Re	Reynolds number	-
T_b	Bulk temperature	K
T	Temperature	K
u	Bulk velocity (average)	m/s
$\dot{q}$	Wall heat flux	W/m^2
$x_{fd,h}$	Hydrodynamic entry length	m
$x_{fd,th}$	Thermal entry length	m
y+	Dimensionless wall distance $y^+ = \Delta_{y_P}/\nu \sqrt{\tau_w/\rho}$	-
ν	Kinematic viscosity	m^2/s
ρ	Density	kg/m^3
τ_w	Wall shear stress	Pa
ω	Specific dissipation rate	1/s

Subscripts

Symbol	
in	Inlet
l	Local, at a defined position
ln	Logarithmic
m	Mean
out	Outlet
w	Wall
z	Local, at a position that varies with z

References

[1]   Nourin F N and Amano R S, Review of gas turbine internal cooling improvement technology, J. Energy Resour. Technol. Trans. ASME, vol. 143, no. 8, pp. 1–8, 2021, 10.1115/1.4048865

[2]   Jain P K, Lanjewar A, Rana K B, and Meena M L, Effect of fabricated V-rib roughness experimentally investigated in a rectangular channel of solar air heater: a comprehensive review, Environ. Sci. Pollut. Res., vol. 28, no. 4, pp. 4019–4055, 2021, 10.1007/s11356-020-11415-6

[3]   Jain S K, Das Agrawal G, and Misra R, A detailed review on various V-shaped ribs roughened solar air heater, Heat Mass Transf. und Stoffuebertragung, vol. 55, no. 12, pp. 3369–3412, 2019, 10.1007/s00231-019-02656-4

[4]   Huynh D and Mahjoob S, Numerical Analysis of Structured Ribbed Channels for Electronic Cooling Applications, Intersoc. Conf. Therm. Thermomechanical Phenom. Electron. Syst. ITHERM, vol. 2020-July, pp. 766–771, 2020, 10.1109/ITherm45881.2020.9190181

[5]   D Fustinoni et al 2012 J. Phys.: Conf. Ser. 395 012042, 10.1088/1742-6596/395/1/012042

[6]   D Fustinoni et al 2015 J. Phys.: Conf. Ser. 655 012060, 10.1088/1742-6596/655/1/012060

[7]   D Fustinoni et al 2017 J. Phys.: Conf. Ser. 796 012015, 10.1088/1742-6596/796/1/012015

[8]   Niro A, Gramazio P, Vitali L and Fustinoni D, Local and global heat transfer characteristics inside a rectangular channel of 1:10 aspect-ratio with ribbed surfaces, International Heat Transfer Conference, pp. 5509-5516, 2018, 10.1615/IHTC16.hte.023149

[9]   Sharma S K and Kalamkar V R, Computational Fluid Dynamics approach in thermo-hydraulic analysis of flow in ducts with rib roughened walls - A review, vol. 55. Elsevier, 2016, 10.1016/j.rser.2015.10.160

[10]   Liu J, Hussain S, Wang J, Wang L, Xie G and Sundén B (2018). Heat transfer enhancement and turbulent flow in a high aspect ratio channel (4:1) with ribs of various truncation types and arrangements. International Journal of Thermal Sciences, 123, 99–116, 10.1016/j.ijthermalsci.2017.09.013

[11]   Saidi A, SundÉn B (2000) Numerical Simulation Of Turbulent Convective Heat Transfer In Square Ribbed Ducts, Numerical Heat Transfer: Part A: Applications, 38:1, 67-88, 10.1080/10407780050134974

[12]   Wei Peng, Pei-Xue Jiang, Yang-Ping Wang , Bing-Yuan Wei. Experimental and numerical investigation of convection heat transfer in channels with different types of ribs Applied Thermal Engineering 31 (2011) 2702-2708, 10.1016/j.applthermaleng.2011.04.040

[13]   Pope S, (2000). Turbulent Flows. Cambridge: Cambridge University Press. doi:10.1017/CBO9780511840531

[14]   Corti M, Gramazio P, Fustinoni D, Vitali L, and Niro A. Accuracy in evaluating heat transfer coefficient by RANS CFD simulations in a rectangular channel with high aspect ratio – Part 1: benchmark on a channel with plane walls, submitted to Journal of Physics Conference Series